Sociedad Mexicana de Ingeniería Mecánica
Fecha de recepción: 03-07-08
Fecha de aceptación: 22-08-08

INGENIERÍA MECÁNICA
TECNOLOGÍA Y DESARROLLO
Vol. 3 No. 1 (2008) 029 - 036

On the Interface Stiffness in Rough Contacts Using Ultrasonic Waves

[1]**Miguel González Valadez**
[2]**Rob S. Dwyer-Joyce**
[1]CIATEQ, A.C., Gerencia de Turbomaquinaria,
Parque Industrial Bernardo Quintana, El Marqués, Querétaro., México
miguel.gonzalez@ciateq.mx , govm740508@hotmail.com
[2]Department of Mechanical Engineering,
The University of Sheffield, Sheffield, UK.
r.dwyerjoyce@sheffield.ac.uk

Abstract

The study proposes the use of a simple spring model that relates the interfacial stiffness with the complex reflection coefficient of ultrasound in a rough contact. The spring model can not be readily related to the real area of contact as this depends on the amount, shape and distribution of contacting asperities. However, it is clear that the model is a powerful non destructive tool to evaluate in an easier way both longitudinal and shear interfacial stiffnesses and its ratio.
The experimental findings agree well with some theoretical predictions evaluated previously and also corroborate the ultrasonic results found in other studies.

Resumen

El estudio propone la utilización de un modelo de resorte simple que relaciona la rigidez interfacial con el coeficiente de reflexión del ultrasonido en un contacto rugoso. El modelo de resorte no puede ser directamente relacionado al área real de contacto, ya que esta depende del número, forma y distribución de las asperezas en contacto. Sin embargo, es claro que el modelo es una poderosa herramienta no destructiva para evaluar en una forma sencilla ambas rigideces normal y cortante y su coeficiente.
Los hallazgos experimentales concuerdan bien con algunas predicciones teóricas evaluadas previamente y también corroboran los resultados de ultrasonido encontrados en otros estudios.

Keywords:
Rough contact, interfacial stiffness, Poisson´s ratio, ultrasonic

Palabras Clave:
Contacto rugoso, rigidez interfacial, razón de Poisson, ultrasonido

Introduction

The interfacial stiffness, produced when a pressure is applied on a pair of contacting rough surfaces, is the ratio of the increase of the contact pressure to the decrease in the surface separation [1, 2]. Interfaces of rough contact will necessarily reduce the overall stiffness of a mechanical component. The interface stiffness also plays a significant role in the static and dynamic analysis of complex structures having joints and elements in sliding contact.

When two rough surfaces are pressed together they really contact in very few asperities. As a consequence, a very high normal stress is undergone by the individual asperities tips, appearing an immediate plastic deformation and forming cold-welded junctions between the metal surfaces. With the application of normal loading-unloading cycles to a rough contact, a phenomenon of hysteresis provoked by plastic deformation has been observed in many experiments [3, 4].

The application of a normal load along with the strength in shear of the contacting junctions, produce a transmission of tangential force between the surfaces; the limiting friction force is that required to rupture the junctions [5]. An objective of this paper is to asses the ratio of the tangential stiffness to the longitudinal stiffness and evaluate whether this ratio is solely affected by the Poisson ratio of the involved materials.

Several theoretical approaches have been developed that can be applied to the contact between two nominally flat surfaces, one of which is smooth and hard and the other rough with isotropic geometry of roughness [1, 6, 7, 8]. As the models work for idealized shape of asperities, they can give an estimation of the real area of contact and nominal pressure. The analysis carried out by Krolikowski & Szczepek [9] which combines the contact model of Greenwood & Williamson with the equation of Johnson [10] for small tangential displacement, revealed that the ratio of tangential to longitudinal stiffness is solely dependent on the Poisson ratio of the contacting rough surfaces. In the same way, but using the equation of Hisakado & Tsukizoe [11] for small tangential displacements of contacting asperities, Sherif & Kossa [12] also concluded that the ratio of stiffnesses can be calculated only from the Poisson ratio of both surfaces in contact.

A more precise theoretical model is that one shown by Baltazar et al. [13]. In their paper, the same equation (only af-

fected by a correction factor accounting for the angle of misalignment) previously obtained by Krolikowski & Szczepek [9] and Mindlin [14] is shown. Predictions of this model are very close to those made through the Sherif & Kossa equation. Additionally, it explains why a slight increase in the ratio of stiffnesses is observed on increasing nominal pressure. The model is again non dependent on the distribution of contact asperities. Yoshioka & Sholtz [15] provide a comprehensive model of elastic contact that allows for the oblique contact in both the normal and shear directions. Nagy [16] have worked with the original approach of the model of Yoshioka & Sholtz [15] for a chi squared distribution of asperities. It was found that the ratio of tangential to longitudinal stiffness is exclusively dependent on the Poisson ratio of the contacting materials.

The development of experimental tools to investigate rough contact has been a very slow process. The methods of electrical conduction, thermal conduction, measurement of fluid flow through the contact and the neutron-graphic method are with certain limitations useful to calculate real contact area but can not be utilized in the estimation of interfacial stiffness [17]. Kendall & Tabor [18] have found different drawbacks with the first two methods as well as with optical methods when used in real engineering contacts. When two nominally flat specimens are pressed together by normal force, the deformation of asperities can be recorded by means of an electric micrometer or by the stylus of a profilometer. The results have to be refined by eliminating the effect of deformation of parts of the test machine. Krolikowski & Szczepek [17] knowledge, however, that the measurable limit of interfacial stiffness of a rough contact is about 1 GPa μm^{-1}.

From the original independent investigations carried out by Kendall & Tabor [18] and Tattersal [19], it was clear that the reflection coefficient of ultrasound can be readily related by means a spring model to the interfacial stiffness of a rough contact and not to the real contact are as it was hypothesized in the study. This finding was seen as a serious disadvantage of the method, however, can be a powerful tool in investigations in which the stiffness is the main parameter to assess. In this paper the ratio of tangential to normal stiffness is evaluated utilizing the spring model of Kendall & Tabor [18].
There are at least two more attempts to explain the ratio of shear to longitudinal stiffness that implies the use of ultrasound, one carried out by Krolikowski & Szczepek [9] and the other by Baltazar et al. [13]. The approach of Krolikowski & Szczepek [9] depends on the modulus and phase shift for both shear and longitudinal waves, parameters that in turn need a previous calculation of stiffness and the coefficient of viscous friction occurring during the rough contact. They found a good agreement between experimental and theoretical results even though the computation process is somehow complicated. An alternative method based on the reflection spectra is that designed by Baltazar et al. [13] using a spring model to infer in a reverse way both shear and longitudinal stiffness. They obtained good agreement on comparing their experimental results with theoretical.

Theoretical

Krolikowski and Szczepec [9] provide a mathematical formulation that takes into account the Hertz-Mindilin theory and the contact model of Greenwood and Williamson. The method models the complex contact between rough surfaces as a normally distributed set of elastic spheres contacting against an elastic plane of the same material loaded with a normal force P and a tangential force S [5, 14, 20]. Both mean contact pressure P, and mean tangential stress τ, are as follow,

$$P = D_s \frac{2E}{3(1-\nu^2)} R^{1/2} \sigma^{3/2} \int_t^{\infty} (x-t)^{3/2} \varphi(x)\, dx \qquad (1)$$

$$\tau = sD_s \frac{2E}{(2-\nu)(1+\nu)} R^{1/2} \sigma^{1/2} \int_t^{\infty} (x-t)^{1/2} \varphi(x)\, dx \qquad (2)$$

where D_s is the summit density per unit area, R is the radius of curvature of the elastic sphere, E is Young's modulus, ν is the Poisson's ratio, σ is the variance of summit height distribution, x is the normalised height of summits, t is the normalised separation and $\phi(x)$ is the normalised height distribution function of the summits.

Thus, the normal, K_σ, and tangential, K_τ, stiffness per unit area for this model are

$$K_\sigma = -\frac{1}{\sigma}\frac{dP}{dt} = D_s \frac{E}{1-\nu^2} R^{1/2} \sigma^{1/2} \int_t^{\infty} (x-t)^{1/2} \varphi(x) dx \qquad (3)$$

$$K_\tau = \frac{d\tau}{ds} = D_s \frac{2E}{(2-\nu)(1+\nu)} R^{1/2} \sigma^{1/2} \int_0^{\infty} (x-t)^{1/2} \varphi(x) dx \qquad (4)$$

Combining Equations (3) and (4) yields the tangential to the normal contact stiffness ratio

$$\frac{K_\tau}{K_\sigma} = \frac{A(1-\nu)}{(2-\nu)} \qquad (5)$$

With A=2, which is also identical with that for the elementary contact previously formulated by Mindlin [14] and more recently by Johnson [10] for two spherical bodies in contact. The form of the equation (5) has been corroborated in several studies which differ basically in the values of the coefficient A. For instance Sherif & Kossa [12] found a theoretical value for $A=\pi/2$. For the model of Yoshioka & Sholtz [15], Nagy [16] obtained an approximated value for $A\approx 0.71$. In the model presented by Baltazar et al. [13], A has a changing value expressed as:

$$A = \frac{2\xi}{\psi} \qquad (6)$$

Where ξ and ψ are correction factors accounting for the geometrical misalignments respect to shear and longitudinal

directions, respectively [21]. The factor ψ takes values about 1 for angles below 50° assuming non-slip condition at the asperities. The factor ξ typically varies between 0.6 and 0.8.

Ultrasonic Response of a Rough Surface Contact

Figure 1a schematically shows the reflection of a sound wave from a rough surface interface. At a contact region a sound wave would pass through. At an air gap it would be totally internal reflected. The proportion of the amplitude of an incident wave that is reflected is known as the reflection coefficient, R.

Thus for two like materials, the reflection coefficient varies from R=0 for complete contact to R=1 for no contact (i.e. a solid air interface). If the nominal pressure across the interface is increased, asperity tip deformations cause both the interface to close slightly and the real area of contact to increase. Kendall and Tabor [18] showed that, when the wavelength of the ultrasonic wave is large compared with the size of the asperity contacts, the reflection is a function of the stiffness of the interface, K. A simple quasi-static spring model ensues (shown schematically in figures 1b and 1c):

$$R = \frac{1}{\sqrt{1+\left(\frac{2K}{\omega z}\right)^2}} \qquad (7)$$

Drinkwater et al. [24] demonstrated that the stiffness of a range of contacts of varying roughness is well represented by equation (7). They studied the reflection as a function of the frequency of the ultrasonic wave. The reflection coefficient was shown to be dependent on frequency, but the predicted stiffness was shown to be independent of frequency.

Experimental SET-UP

Figure 2 shows the loading frame and the arrangement of the ultrasonic equipment used in the tests. Two synchronized ultrasonic pulser-receivers were arranged to make possible that longitudinal and shear signals were simultaneously processed. The specimens were subjected to loading-unloading cycles of compressive pressure in a hydraulic frame operating in load control mode. The upper specimen had a disk of piezoelectric material glued to the back face with a temperature stable contact adhesive. The transducer was of the wrap around electrode type so both wires could be soldered directly to the top face of the ≈5MHz centre frequency transducer. The lower specimen was interrogated by means of a 5MHz longitudinal wave planar contact transducer. The upper specimen was loaded against the lower specimen, through an annulus with a hemispherical cap. The hemispherical end piece allowed the upper specimen to align against the lower and then obtain a more distributed and conformed contact.

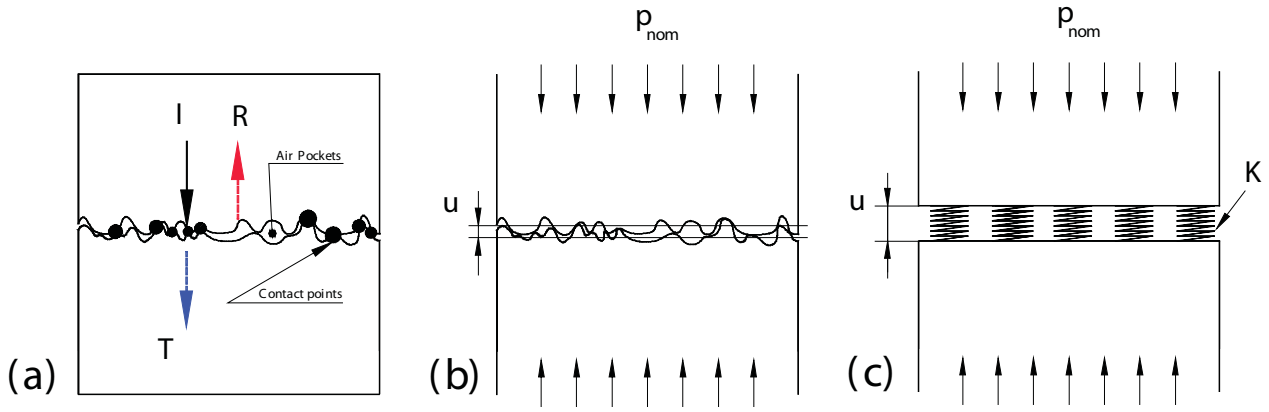

Fig. 1. Scheme showing a representation of the ultrasonic response of rough surface contact, a) reflection, b) loading and deflection, and c) the spring model representation.

Where z is the acoustic impedance of the material either side of the interface and ω is the angular frequency of the ultrasonic wave. The relationship holds for both longitudinal and shear wave reflections (the longitudinal and shear wave speeds are used, respectively). A similar expression exists for two dissimilar materials pressed together [22]. This model has been used extensively to study the reflection and transmission of sound across incomplete interfaces [4, 16, 17, 23].

The contacting interfaces were made from steel specimens (see Table 1). The contacting face of the bottom specimens were ground and polished, whilst those of the upper specimens were grit-blasted (see Figure 3). All surfaces were measured using a surface profilometer before and after the loading experiments (Table 2).

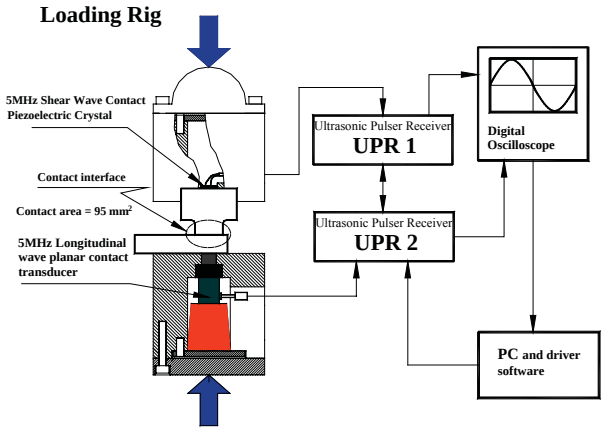

Fig. 2. Schematic diagram showing loading rig, specimens and ultrasonic measuring apparatus.

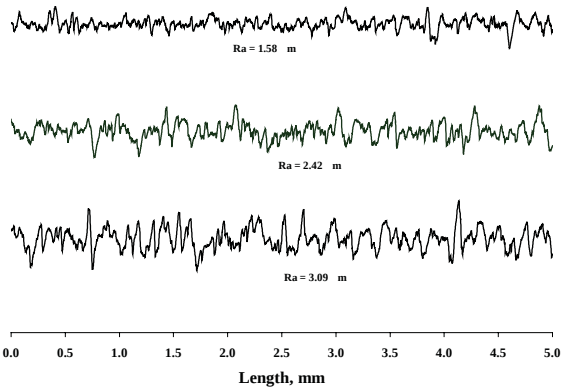

Fig. 3. Different grit blasted upper specimens used in the experiment.

Steel	Elements weight %								Density, kg/m3	Young Modulus, GPa	Poisson´s Ratio
	C	Mn	P	S	Si	Cr	Ni	Mo			
A I S I 4340	0.38-0.43	0.60-0.80	0.035 (max)	0.04 (max)	0.15-0.30	0.70-0.90	1.65-2.00	0.20-0.30	7.7-8.03	190-210	0.27-0.30

Table 1. Steel properties for experimental contact interfaces, taken from Engineering Fundamentals, EFUNDA 2008 [25]

Material	Ra in upper specimens		Ra in bottom specimens	
	Before Loading	After Loading	Before loading	After Loading
Grit-blasted steel 1	1.58	1.18	0.03	0.07
Grit-blasted steel 2	2.42	1.52	0.04	0.16
Grit-blasted steel 3	3.09	1.82	0.04	0.13

Table 2. Roughness before and after test (sample length 5 mm, each result is an average of three profiles). Both specimens are made up of steel.

Two synchronized ultrasonic pulser-receivers (UPR) were used to generate voltage pulses to actuate the transducers. Both shear and longitudinal transducers had a centre frequency of 5 MHz. The reflected pulses were received by the digital oscilloscope, amplified, and passed to the PC for signal processing.

Before both specimens are pressed together, a reference signal of ultrasound is taken. This signal is taken in the point where no contact exists at all. In these cases the entire incident waves, shear and longitudinal, at the interface are reflected completely (and virtually none is transmitted at the metal-air interface). The assumption that the incident wave fully reflects in an interface of solid-air, is backed by the fact that air poses very low acoustic impedance (400 Ns/m3), as opposed to steel (47x106 Ns/m3). This is the reason why air is considered as a pure reflector or mirror to ultrasound. These signals are therefore equivalent to the incident signals, and are used as a reference pulses

The test specimens are then loaded together and subsequent reflected pulses are recorded. The load is applied gradually by steps until reaching a maximum nominal pressure of 400MPa. The loading steps consist basically in applying the load from zero to the maximum with a tension-compression machine. Conversely, the unloading process is executes by decreasing the load from the maximum value down to a low load of 5MPa. It should be ensured that the contact interface do not be downloaded completely as this would involve a different set of asperities to come into contact in the next loading-unloading cycle.

A Fourier transform is performed on both the reflected and reference signals; dividing one by the other gives the reflection coefficient spectrum. For a rough surface interface this reflection coefficient depends on the frequency. Equation (7) is then used to obtain the interfacial stiffness which should be independent of frequency. In practice, there is a little statistical variation due to noise in the signal, and a mean stiffness is determined for all frequencies within the transducer bandwidth.

More details of this method for determining interface stiffness ultrasonically can be found in Dwyer-Joyce et al. [4].

Results

Figures 4, 5 and 6 show the experimental results. Both interfacial stiffnesses, shear and longitudinal were calculated with equation (7). Both acoustical impedances z, for shear and longitudinal waves were calculated from typical values of speed of sound for steel of 5900 m/s and 3100 m/s, respectively [26]. It can be observed that the normal stiffness during the loading step of the first cycle in terms of normal pressure follows an approximate linear relationship [27, 28]. This behavior has previously provided a simple calibration route for maps of contact stiffness and other studies [29]. It is clear that to predict the normal pressure from stiffness measurement in a contacting joint, their roughness had to be reproduced in laboratory specimens and the predictions would only useful for the first loading.

The curve of the unloading process in all cases follows a different path than that of the loading step showing a hysteresis phenomenon. This also indicates that most of the asperity plasticity has been achieved at this stage. It is been previously recognized that the first loading on the contact interface always surpass the elasticity of asperities and therefore occurs in elasto-plastic conditions [30]. The ultrasound is not strongly affected by the plasticity of the contact, and it depends basically of the increase of contact area with load.

After the first loading-unloading cycle, and to make sure that remaining plasticity is fully removed and the contact is occurring in elastic conditions, 10 more complete cycles were applied. Under these conditions, the normal and shear deformations are caused by the passage of a very small displacement wave, which causes only elastic deformation.

In figures 4, 5 and 6 for simplicity only the curves of the loading step of cycle 11 are shown. It is important to notice that one could use either the loading curve or unloading curve as the values are basically the same. The values of stiffness are higher for the contact interface with the least roughness. In the three different samples the shear stiffness produces similar curves than those of normal stiffness.

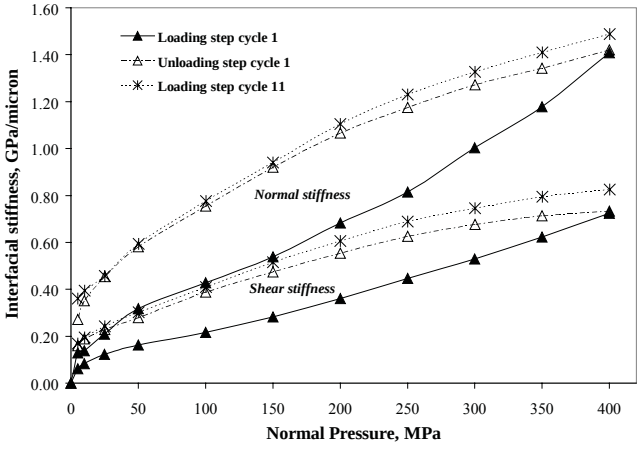

Fig. 4. Normal pressure vs. interfacial stiffness for a steel-steel interface. The upper specimen had a roughness value before test, Ra=1.58 μm.

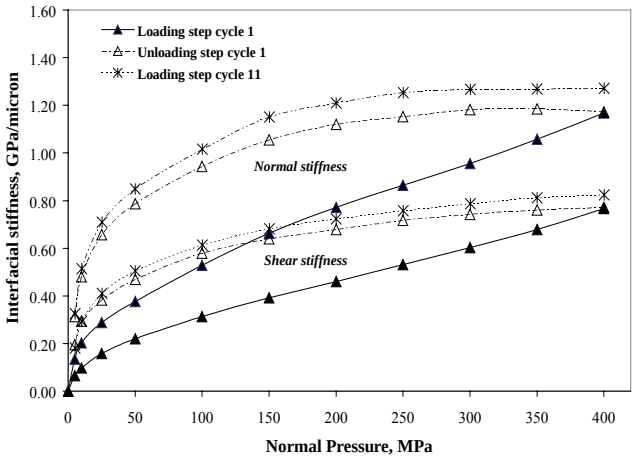

Fig. 5. Normal pressure vs. interfacial stiffness for a steel-steel interface. The upper specimen had a roughness value before test, Ra=2.42 μm.

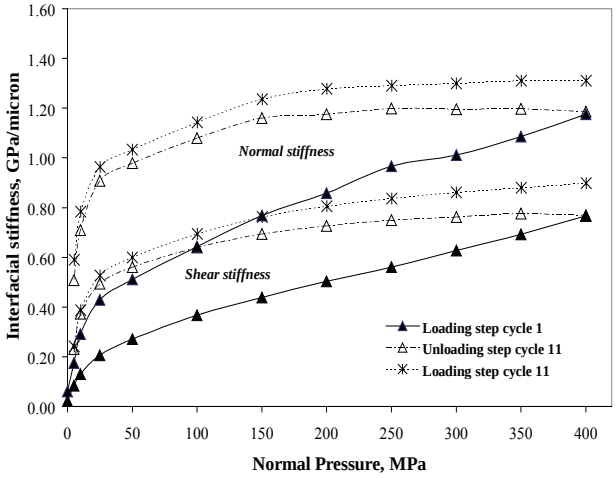

Fig. 6. Normal pressure vs. interfacial stiffness for a steel-steel interface. The upper specimen had a roughness value before test, Ra=3.09 μm.

Analysis and Discussion

Figures 7, 8 and 9 show plots of longitudinal stiffness against shear stiffness. In addition, the theoretical predictions found in previous literature are used to compare the experimental results. For the comparison data from the loading step of cycle 1 and loading step of cycle 11 were used. This is to get insight of what happens in an elasto-plastic contact (first loading-unloading cycle) and in a pure elastic contact (eleventh loading-unloading cycle). To calculate the theoretical predictions equation (5) with a Poisson ratio ν=0.3 was used. The ratio between the two stiffness values is virtually linear over the entire loading range for both elasto-plastic contact and pure elastic contact. This indicates that there is a fixed relationship (i.e. load independent ratio) between normal and shear stiffness. The experimental results show a linear behavior with a slope very close to the theoretical predictions of Sherif & Kossa [12] and Baltazar et al. [13] with an average value of the correction factor ξ=0.7 which also suggests that the stiffness ratio is strongly dependent on Poisson´s ratio. In the plots of figures 7, 8 and 9 is also observed that the equation

in Krolikowski & Szczepek [9] over predicts the experimental findings of our study ($(K_\tau/K_\sigma \approx 0.82$). In contrast, the model of Yoshioka & Scholz [15] predicts values significantly lower than experimental data ($K_\tau/K_\sigma \approx 0.29$). In a previous study carried out by Dwyer-Joyce & Gonzalez-Valadez [31], it was found that ultrasonic results agreed well with the model of Yoshioka & Scholz. However, during the tests there was a serious difficulty to keep the contacting surfaces properly aligned; this in turn produced erroneous stiffness measurements.

In order to have a more realistic comparison between models that work for interfacial elastic contact and ultrasonic results, only data from the eleventh cycle have been plotted in Figure 10. As it can be observed, the theoretical data is non dependent on normal pressure. It is important to note that surfaces with smaller roughness, and therefore, with flatter profiles, have lower value of the ratio $K_\tau K_\sigma$. An unusual behavior is observed at the lower loads (up to 50MPa). In this range a bigger slope than that found for loads above 50MPa was found. It is not completely clear what is causing this, but can be attributable partially to the fact that at this level of load the interfacial contact is still conforming and/or aligning and the readings can somewhat be affected.

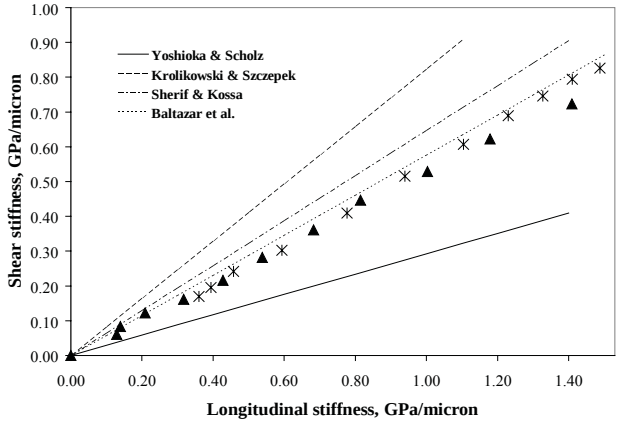

Fig. 7. Longitudinal stiffness vs. shear stiffness in a contact interface with a roughness value before test of Ra=1.58 µm on the upper specimen.
▲Experimental data from loading step of cycle 1.
✳Experimental data from loading step of cycle 11.

The ultrasonic values of the ratio of stiffnesses for the three levels of roughness show curves very close to the constant theoretical predictions found in Sherif & Kossa [12] and in Baltazar et al. [13]. In the plot of Figure 10, constant prediction by Baltazar et al. [13] has been done with an average correction factor ξ=0.7. According to theoretical models, a constant value of K_τ/K_σ respect to normal pressure should be expected. However, in the ultrasonic data of Figure 10, a slight constant increase in the ratio with load is observed what suggests that some factor or factors other than the Poisson ratio could be involved. A similar tendency was obtained by Baltazar et al. [13], who intuitively deducted that an increase of normal pressure is related to an increase in the misalignment angle. As a consequence, the correction factor ξ should not be taken as a constant value. This is not visible in Figure 10 as theoretically is not possible to predict the change of K_τ/K_σ in terms of normal pressure only by using equations (5) and (6), however this change is experimentally corroborated.

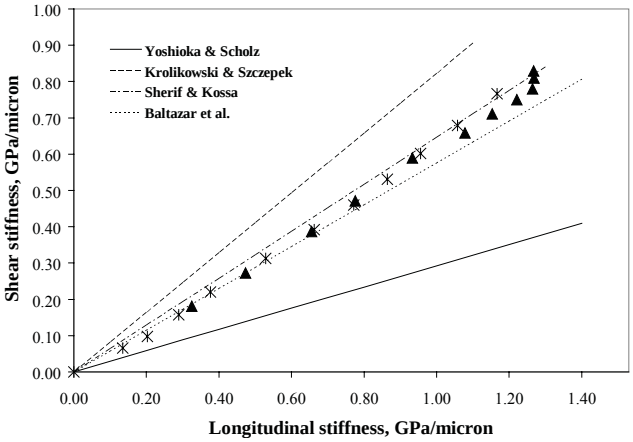

Fig. 8. Longitudinal stiffness vs. shear stiffness in a contact interface with a roughness value before test of Ra=2.42 µm on the upper specimen.
▲Experimental data from loading step of cycle 1.
✳Experimental data from loading step of cycle 11.

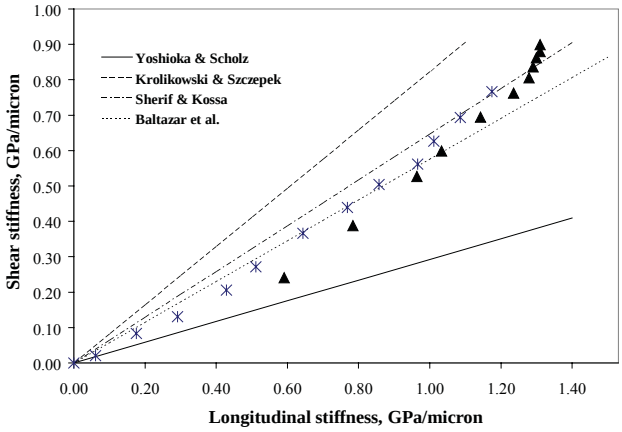

Fig. 9. Longitudinal stiffness vs. shear stiffness in a contact interface with a roughness value before test of Ra=3.09 µm on the upper specimen.
▲Experimental data from loading step of cycle 1.
✳Experimental data from loading step of cycle 11.

That the ratio of shear to longitudinal stiffness shows a slightly increase with load makes the method not completely useful to predict the Poisson´s ratio of the contacting materials as the variation of correction factors ξ and ψ with load need to be determined.

Conclusions

An ultrasonic approach has been used to determine the normal and shear stiffness for three different grit-blasted surface contacts. The spring model to calculate and compare interface stiffness in terms of reflection of ultrasound proved to be reliable and more direct than existing methods.
Shear and normal stiffness follow similar behaviour in elastic

and plastic conditions. The ratio K_τ/K_σ is not strongly dependent on roughness.

Experimental data agree well with those theoretical models that predict values of the ratio of stiffnesses K_τ/K_σ in a range between 0.5 and 0.7. However not a fixed ratio was found what suggested that more parameters other than Poisson´s ratio require to be analyzed.

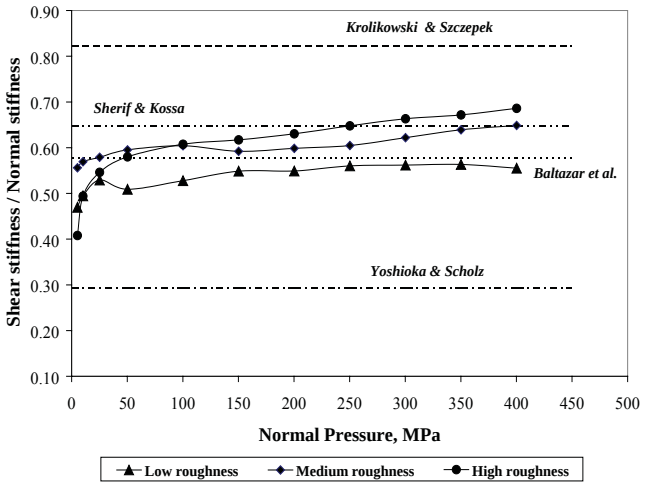

Fig. 10. Normal pressure vs ratio of shear to normal stiffness for the three different contact interfaces.

Referencias

1. A.W. Bush, R.D. Gibson, T.R. Thomas, The elastic contact of a rough surface, Wear 35 (1975) 87-113.

2. T.R. Thomas, R.S. Sayles, Stiffness of machine tool joints: a random-process approach, ASME Journal of Engineering for Industry 99 B1 (1977) 250-256.

3. D. Tabor, The Hardness of Metals, Oxford University Press, USA, 2000, p.192.

4. R.S. Dwyer-Joyce, B.W. Drinkwater, A.M. Quinn, The use of ultrasound in the investigation of rough surface interfaces, ASME Journal of Tribology 123 (2001) 8-16.

5. J.J. O´Connor, K.L. Johnson, The role of surface asperities in transmitting tangential forces between metals, Wear 6 (1963) 118-139.

6. J.A. Greenwood, J.B.P. Williamson, 1966. Contact of nominally flat surfaces, Proceedings of the Royal Society of London: Series A 295 (1966) 300-319.

7. D.J. Whitehouse, J.F. Archard, The properties of random surfaces of significance in their contact, Proceedings of the Royal Society of London: Series A 316 (1970) 97-121.

8. R.A. Onions, J.F. Archard, The contact of surfaces having a random structure, Journal of physics, D: Applied Physics 6 (1973), 289-304.

9. J. Krolikowski, J. Szczepek, Assessment of tangential and normal stiffness of contact between rough surfaces using ultrasonic method, Wear 160 (1993) 253-258.

10. K.L. Johnson, Contact Mechanics, Cambridge University Pres, New York, 1987, p.464.

11. T. Hisakado, T. Tsukizoe, Effects of distribution of surface slopes and flow pressures of contact asperities on contact between solid surfaces, Wear 30 (1974) 213-227.

12. H.A. Sherif, S.S. Kossa, Relationship between normal and tangential contact stiffness of nominally flat surfaces, Wear 151 (1991) 49-62.

13. A. Baltazar, S.I. Rokhlin, C. Pecorari, On the relationship between ultrasonic and micromechanical properties of contacting rough surfaces, Journal of the Mechanics and Physics of Solids 50 (2002) 1397-1416.

14. R.D. Mindlin, Compliance of elastic bodies in contact, Journal of Applied Mechanics 71 (1949) 259-268.

15. N. Yoshioka, C.H. Scholz, Elastic properties of contacting surfaces under normal and shear loads: Part 1 – Theory, Journal of Geophysics Research 94 (1989) 17681-17690.

16. P.B. Nagy, Ultrasonic classification of imperfect interfaces, Journal of Nondestructive Evaluation 11 (1992) 127-139.

17. J. Krolikowski, J. Szczepek, Prediction of contact parameters using ultrasonic method, Wear 148 (1991) 181-195.

18. K. Kendall, D. Tabor, An ultrasonic study of the area of contact between stationary and sliding surfaces, Proceedings of the Royal Society of London: Series A 323 (1971) 321-340.

19. H.G. Tattersall, The ultrasonic pulse-echo technique as applied to adhesion testing, Journal of Applied Physics: Part D 6 (1973) 819-832.

20. M. Raoof, R.E. Hobbs, Tangential compliance of rough elastic bodies in contact, ASME Journal of Tribology 111 (1989) 726-729

21. K.Yamada, N. Takeda, J Kagami, T. Naoi, Mechanisms of elastic contact and friction between rough surfaces, Wear 48 (1978) 15-34.

22. M. Schoenberg, Elastic wave behavior across linear slip interfaces, Journal of the Acoustical Society of America 68 (1980) 1516-1521.

23. N.F. Haines, The theory of sound transmission and reflection at contacting surfaces. Report RD/B/N4744, CEGB Research Division, Berkeley Nuclear Laboratories, 1980.

24. B.W. Drinkwater, R.S. Dwyer-Joyce, P. Cawley, A study of the interaction between ultrasound and a partially contacting solid-solid interface, Proceedings of the Royal Society: Series A 452 (1996) 2613-2628.

25. EFUNDA, Engineering Fundamentals, in: www.efunda.com, 2008.

26. J. Krautkramer, H. Krautkramer, Ultrasonic Testing of Materials, Springer-Verlag, Fourth Edition, 1990, p.677.

27. T. Arakawa, A study of the transmission and reflection of an ultrasonic beam at machined surfaces pressed against each other, Materials Evaluation 41 (1983) 714-719.

28. K. Hodgson, The Use of Ultrasound to Investigate Engineering, Doctoral Thesis, The University of Sheffield, UK, 2002.

29. M.B. Marshall, R. Lewis, B.W. Drinkwater, R.S. Dwyer-Joyce, An approach for contact stress mapping in joints and concentrated contacts, Journal of Strain Analysis 39 (2004) 339-350.

30. J.Y. Kim, A. Baltazar, S.I. Rokhlin, Ultrasonic assessment of rough surface contact between solids from elastoplastic loading-unloading hysteresis cycle, Journal of the Mechanics and Physics of Solids 52 (2004) 1911-1934.

31. M. Gonzalez-Valadez, R.S. Dwyer-Joyce, Ultrasonic determination of normal and shear interface stiffness and the effect of poisson´s ratio, In the Proceedings of the 30th Leeds-Lyon Symposium on Tribology, Elsevier Tribology Series 43, pp, 143-150, 2004.